
CHAPTER 22

SPACE-BASED RADAR SYSTEMS AND TECHNOLOGY

Leopold J. Cantafio
Space and Technology Group TRW

22.1 INTRODUCTION

Significant developments have been made in space-based radar (SBR) systems and technology since the 1970 edition of the *Radar Handbook* was published. A new rendezvous radar was developed for the space shuttle and has become operational. The unmanned orbital maneuvering vehicle (OMV) will use a new low-cost rendezvous radar that is expected to be operational during the early 1990 time period. Synthetic aperture radar (SAR) types of SBR have been used for earth and planetary exploration. Altimeters have been used on many satellites. The technology of SBR subsystems has been developed in the areas of antennas, transmitters, receivers, solid-state transmit-receive (T/R) modules, signal processors, and prime power. This chapter will review SBR systems and technology with the intent to provide a description that is not too sketchy to be substantive. Therefore, selected systems and technology will be discussed. Several SBR systems for rendezvous, earth exploration, and planetary exploration missions will be described. Systems considerations such as the space environment, orbit selection, radar tradeoffs, advantages and disadvantages, and critical issues will be discussed. Many topics, such as electronic countermeasures, will have to be omitted. This chapter should be considered a status report on the new frontier for radar systems. A more comprehensive treatment of SBR can be found in "Spacebased Radar Handbook," written and edited by the author and published by Artech House.

22.2 SBR SYSTEMS CONSIDERATIONS

Types of SBR. There are three types of radar that have been and can be based in space. SBR that is typical of Type I is the small, short-range rendezvous radar such as those used on the Shuttle, Apollo, and Gemini programs.¹⁻⁴ Type II SBR includes the earth and planetary resources radar used for mapping, scatterometers, altimeters, and subsurface probing.⁵⁻⁹ Side-

looking SAR techniques are typical of mapping radars such as those used on the Seasat satellite in June 1978 and the Shuttle in November 1981 with the Shuttle Imaging Radar-A (SIR-A). Type III SBR includes the large phased array surveillance radar proposed for multimission defense, air traffic control, and disarmament functions.¹⁰⁻¹⁴

Type I SBR. Gemini and Apollo programs demonstrated the first operational experience with the rendezvous maneuver. The successful performance of the rendezvous radars in these programs effectively opened the door to many possible missions that may be performed in space. The K_u -band integrated radar and communications subsystem (IRACS), designed for the space shuttle orbiter vehicle, demonstrated the rendezvous, satellite retrieval, and station-keeping missions. The maiden voyage for this radar was aboard *Challenger* (Shuttle) STS-7 on June 22, 1983.¹⁵ During the STS-11 flight in February 1984, the K_u -band radar assisted in the checkout of the manned maneuvering unit (MMU) operations. The radar acquired and tracked mission specialist Robert Stewart in the MMU during his 300-ft sojourn into space. The radar measured the radar cross sections (RCS) of the MMU, which varied between 2.5 and 7.5 dBsm with acquisition at a range of 100 ft and track out to the maximum range of 308 ft. Average velocity during the mission was 0.7 ft/s.

The rendezvous radar provides the tracking function for a guidance system. The rendezvous phase of the mission begins after the radar acquires the target. Thereafter, the tracking function provides data on range, range rate, and the two components of the line-of-sight inertial rate. A digital guidance computer calculates relative velocity perpendicular to the line of sight, using range and angular rate data. The closing component of velocity is obtained from the doppler or by differentiation of radar range measurements. A simplified block diagram of a typical rendezvous guidance subsystem is shown in Fig. 22.1. The radar search and acquisition mode is initiated by the guidance computer. A relatively large solid angle is searched periodically until the target is acquired in range and angle. In order to maximize the probability of detection and acquisition, the kinematics are arranged such that a long search time is available before the target escapes from

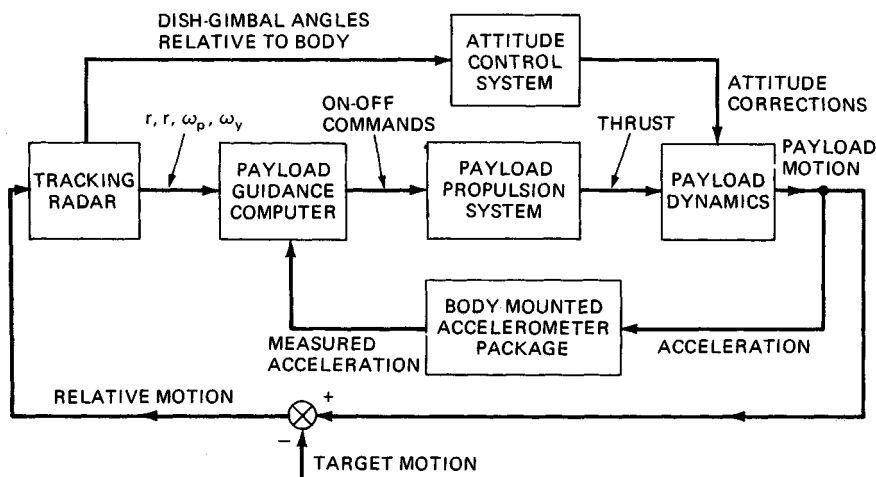


FIG. 22.1 Rendezvous guidance subsystem: simplified block diagram.¹⁶

TABLE 22.1 STS Rendezvous Radar Requirements*

Search	$\pm 30^\circ$ spiral scan
Acquisition	12 nmi on 0 dBsm SW-1; 300 nmi on +14 dBW transponder
Track	
Range	± 1 percent
Range rate	1 ft/s or 1 percent
Angle	8 mrad
Angle rate	0.14 mrad/s or 5 percent

*From Ref. 15.

the search sector. When detection has been accomplished, the search mode is stopped and the tracking mode is initiated by locking a tracking gate onto the target return and thereafter monopulse angle-tracking the antenna about an axis always directed toward the target. The tracking phase ends when rendezvous has been achieved within certain desired terminal accuracy on relative position and velocity. The typical requirements for the STS rendezvous radar are given in Table 22.1.¹⁵

At and immediately following acquisition, the relative velocity vector will generally lie in the direction of the instantaneous line of sight; however, there may be a substantial error equivalent to a relative velocity component perpendicular to the line of sight. The range at acquisition and the magnitude of the closing velocity are such that the rendezvous-phase duration can be several minutes. A reasonably long period is essential to an accurate rendezvous, since sufficient time must be allowed for smoothing the inherently noisy radar tracking data as well as for correcting measured errors. A period of as much as 10 to 20 min is still short compared with the overall mission duration. The effect of the differential earth gravity field has been shown by Hord¹⁷ to be negligible for tracking-phase durations not exceeding 10 to 20 min. Furthermore, Wolverton¹⁶ has shown that when the rendezvous time t_r is small compared with the product of the satellite orbital period T_0 and $(2\pi)^{-1}$, the orbital motion aspects of the rendezvous maneuver can be neglected.

Type II SBR. Remote sensing of the earth from space began in 1960 with the launch of the first television and infrared observation satellite (Tiros) weather satellite. Remote sensing of the earth from space by radar began in 1975 with the launch of the GEOS-C by the National Aeronautics and Space Administration (NASA) and continued with the Seasat in 1978, the SIR-A on the Shuttle in 1981, and the SIR-B on the Shuttle STS-17 in 1984.

SEASAT-A SYSTEM. The Seasat-A program was managed for the NASA Office of Applications by the California Institute of Technology Jet Propulsion Laboratory (JPL). The mission for Seasat-A was to demonstrate that measurements of ocean dynamics are feasible. The measurements included topography, surface winds, gravity waves, surface temperature, sea-ice extent and age, ocean features, and salinity. Precision of the geoid measurement was specified as ± 10 cm.¹⁸

The Seasat-A satellite was launched at 6:12 P.M. PST on June 26, 1978. The orbital altitude was 783 km at apogee and 778 km at perigee. The retrograde polar orbit had an inclination angle of 108° and a period of 100.5 min. Three radar and two radiometer sensors were carried on the spacecraft. The coherent SAR, described in Sec. 22.3, operated at 1.275 GHz. The radar altimeter operated in the 12- to 14-GHz band and covered a 1.6-km swath directly below the spacecraft.

The wind scatterometer operated at 14.599 GHz and covered two swaths, each 400 km wide and offset on each side of the spacecraft. Four antennas were used to measure wind speed in the range from 4 to 28 m/s. The microwave radiometer had five frequency channels at 6.6 GHz, 10.6 GHz, 18 GHz, 21 GHz, and 37.6 GHz. A swath 1000 km wide, centered at the nadir, was covered. The visible and infrared (IR) radiometer covered a single swath 1800 km wide, symmetrical about the nadir.

Seasat-A collected data until Oct. 9, 1978, when a short circuit developed at the slip rings between the solar array and the power distribution bus.

The primary objectives of the SAR experiment on Seasat-A included (a) to obtain radar imagery of ocean wave patterns in deep oceans, (b) to obtain ocean wave patterns and water-land interaction data in coastal regions, and (c) to obtain radar imagery of sea and fresh-water ice and snow cover. The secondary objectives included (a) to obtain radar imagery of land surfaces; (b) to obtain data for mapping of the earth's surface; (c) to obtain data for estimates of land and sea surface roughness, ice type, differentiation of surface materials, vegetation, and landforms; (d) to obtain data for monitoring changes in the environment; (e) to obtain a demonstration of all-weather, day-night measurement capability; and (f) to obtain data useful for designing future high-resolution spaceborne radar systems.

GEOS-3. The Geodynamics Experimental Ocean Satellite (GEOS-3) was a remote-sensing satellite that contained five instruments in the experiment package.¹⁹⁻²¹ These were (1) an SBR altimeter, (2) two C-band transponders, (3) an S-band transponder, (4) laser retroreflectors, and (5) a radio doppler system. The purpose of the GEOS-3 satellite was to perform experiments in support of the application of geodetic satellite techniques to geoscience investigations such as earth physics and oceanography. The SBR altimeter mission objective on the GEOS-3 satellite was to perform an in-orbit experiment that (1) determined the feasibility and utility of a space-borne radar altimeter to map the topography of the ocean surface with an absolute accuracy of ± 5 m and with a relative accuracy of 1 to 2 m, (2) determined the feasibility of measuring waveheight, (3) determined the feasibility of measuring the deflection of the vertical at sea, and (4) contributed to the technology leading to a future operational altimeter satellite system with a 10-cm measurement capability.

The GEOS-C satellite (its designation was changed to GEOS-3 after successful orbit had been achieved) was launched on Apr. 9, 1975. The nominal orbit parameters were as follows: mean altitude, 843 km; inclination angle, 115°; eccentricity, 0.000; and period, 101.8 min. The GEOS-3 spacecraft was an eight-sided aluminum shell topped by a truncated pyramid. The satellite width was 132 cm (53 in), and the height was 81 cm (32 in); the weight of the GEOS-3 was 340 kg (750 lb).

Type III SBR. Before the design of a Type III SBR can begin, requirements for the surveillance radar systems must be specified. These requirements should include but not be limited to²² (1) target radar cross section model, (2) target velocity and acceleration (maximum), (3) number of targets, (4) probability of detection, (5) probability of false alarm and false-alarm time, (6) track accuracy, (7) minimum target spacing, (8) designation error, (9) warning time, (10) length of detection fence, (11) revisit time, (12) clutter model, and (13) weather model. With these requirements as a minimum input to the design study, orbit selection can begin and parameter tradeoffs can be made. The influence of the space environment, interference, and clutter must be considered. Since the Shuttle (STS) can be a major launch vehicle for SBR, its capabilities should be examined. The

advantages and disadvantages of large surveillance radar in space should also be considered.

Target characteristics and requirements for coverage, track data rate, and revisit rate are important parameters. The radar subclutter visibility capability, antenna size, scan rate, and grazing-angle limitations also determine the orbit selected for the SBR. The space environment itself can determine the selected orbit if the natural-radiation lifetime dosage that the SBR electronics receives is too large. Finally, there is the requirement to use the least number of satellites to keep total system cost to a minimum.

Considerations

Orbit Selection. Many factors contribute to the selection of the orbit to be used for each type of SBR and particularly for a large surveillance-type SBR. The orbit parameters of period, altitude, and velocity are the first consideration. The velocity for a satellite in a circular orbit around the earth is given by¹⁶

$$V_c = \sqrt{\frac{\mu}{r}} \quad (22.1)$$

where r is the distance of the satellite from the center of the earth and μ is the product of the universal gravitational constant and the mass of the earth. The period of a satellite of the earth is given by¹⁶

$$T = \frac{2\pi\mu}{\sqrt{V_a^3 V_p^3}} \quad (22.2)$$

where V_a is the velocity of the satellite at apogee and V_p is the velocity of the satellite at perigee. For a circular orbit, $V_a = V_p$ and the period of a circular orbiting satellite is

$$T_c = \frac{2\pi\mu}{V_c^3} \quad (22.3)$$

Table 22.2 shows selected calculations of circular-orbit velocity and period when the radius of the earth is $20.903 (10)^6$ ft, μ is $1.4069 (10)^{16}$ ft³/s², and 1 nmi is 6076.1 ft.

Many studies concerning the design of satellite constellations for optimal coverage have been made and reported.²³⁻²⁸ Luders and Ginsberg²⁴ describe an analytical solution to the problem of achieving continuous coverage of latitudinally

TABLE 22.2 Selected Orbital Parameters

Altitude, nmi	Velocity, ft/s	Period, min
99	25,587	88
414	24,520	100
912	23,074	120
2,262	20,157	180
5,612	15,999	360
19,369	10,079	1,440

bounded zones of the globe. Emara and Leondes²⁷ solved the problem of simultaneous observations by at least four satellites by a constellation of the minimum number of satellites. Ballard²⁵ extended earlier work by Walker²³ and analyzed rosette constellations that provided the largest possible great-circle range between an observer anywhere on the earth's surface and the nearest subsatellite point. Single, double, triple, and quadruple visibility was provided by various constellations. Beste²⁶ designed satellite constellations that provided single and triple continuous coverage by the minimum number of satellites. All these studies determined coverage for satellites with sensors that observe only angles around the nadir. Electro-optical sensors and mapping radars are typical sensors that provide this coverage. However, these studies do not provide results for SBR surveillance sensors that must detect targets in clutter. These sensors typically have a *nadir hole* 20 to 30° off nadir in which the signal-to-clutter ratio (*SCR*) is too large for reliable detection. This is shown in Fig. 22.2 for a 50° maximum grazing angle and a 3° minimum grazing angle. The minimum grazing angle is a limit set by the atmospheric attenuation allocated in the SBR loss budget and the refraction angle error. To illustrate the different results that can be obtained, consider a requirement to provide continuous coverage of the earth from an orbital altitude of 10,371 km (5600 nmi). For a single sensor on each satellite with no grazing-angle limitations, a constellation of six satellites can provide the required continuous coverage from polar orbits. The satellites would be equally distributed in two orbital planes, using the study results given by Harney.²⁸ However, if the sensor in the SBR was limited to grazing angles between 3 and 60°, then the required coverage could be provided by a constellation of 10 satellites. This constellation consists of 1 satellite in each of 10 equally spaced orbit planes at an inclination of 49.4°, resembling the Walker 10/10/8 constellation.²⁵ If the grazing angles extend between 3 and 70°, then a 14-satellite constellation in a Walker 14/14/12 configuration provides a continuous global twofold coverage. The inclination angle of each orbital plane is 49.4°.

Space Environment. For a large phased array type of radar operating in space, the thermal and natural radiation environments have significant influence on the design of an SBR. Particular effects depend on the orbital altitude and the materials used in the structure.

Thermal Environment Effects. In general, distortion of a phased array antenna will cause a decrease in antenna gain. Figure 22.3 shows the effect of random phase errors caused by the distortion ϵ when the error correlation interval is large with respect to a wavelength. It is seen from Fig. 22.3 that a 2 dB loss in gain is obtained when the distortion is about one-tenth of a wavelength. Thus for a 50-m-diameter planar corporate phased array antenna operating at a wavelength of 10 cm, the rms distortion of the plane of the array must be held to less than 1 cm if a 2 dB loss in antenna gain is to be maintained.

Thermal distortion in a 70-ft (21.34-m) diameter parabolic reflector was studied²⁹ at synchronous orbit. Reflector performance comparisons were made for titanium and graphite composite materials. Generally the tolerances that must be held on reflector antennas are more severe than for phased arrays for the same performance. Figure 22.4 shows the results of the analysis. Performance of the

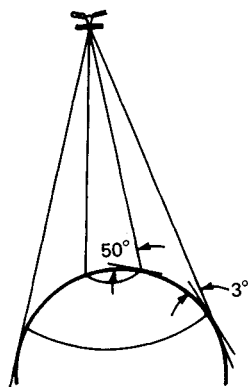


FIG. 22.2 SBR coverage and nadir hole.

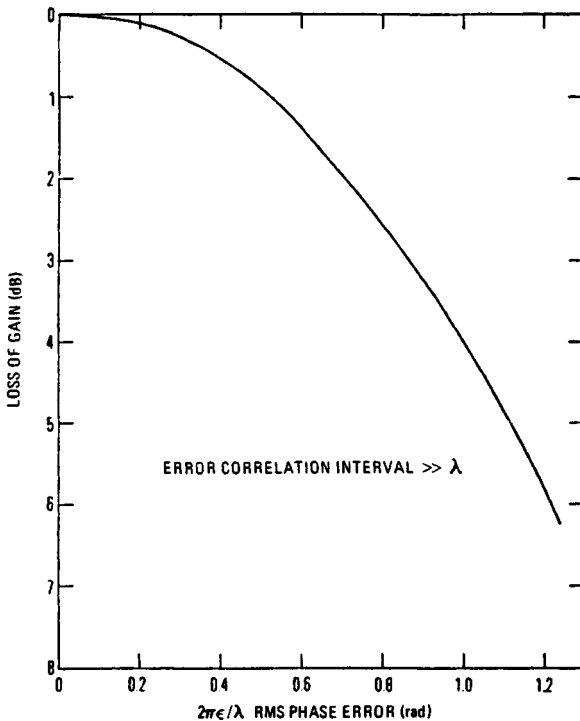


FIG. 22.3 Antenna loss of gain due to random phase errors.

graphite composite material is superior, giving an rms distortion of about 0.076 cm. If this is one-fiftieth of the wavelength, then the antenna could operate satisfactorily at a wavelength of 3.8 cm.

Consider a 70-m-diameter-lens phased array^{30,31} at an altitude of 5600 nmi as shown in Fig. 22.5. The progress of the sun angle is shown. Simulations have predicted the following maximum and minimum temperatures for selected parts of the space-fed lens antenna:

Location	Temperature, K	
	Maximum	Minimum
Ground plane	264	224
Rim	182	160
Upper stays	231	186
Lower stays	217	201
Upper dipole plane	314	201
Lower dipole plane	274	220

By choosing the proper materials, the design of this class of antenna will experience low distortions compared with those allowable. Figure 22.6^{32,33} shows the loss in relative gain for a 71-m-diameter space-fed antenna as a function of the

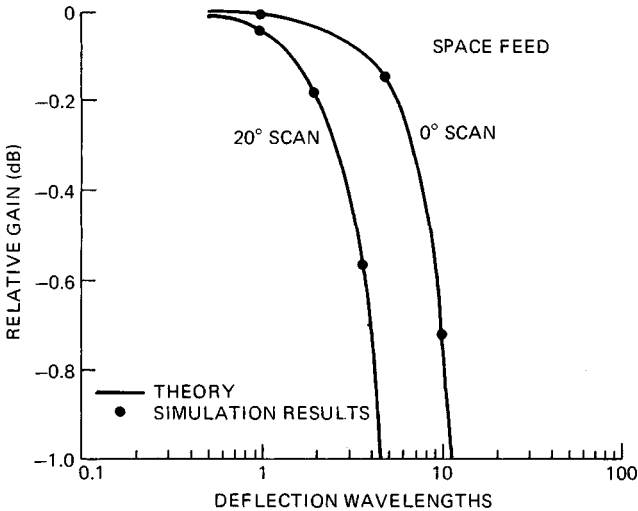


FIG. 22.6 Loss of gain due to distortion for a space-fed array.³²

deflection or distortion in wavelengths. It is seen that the relative gain is down 1 dB when the distortion is about 5 wavelengths at a 20° scan angle.

RADIATION ENVIRONMENT EFFECTS. SBRs can encounter in space particle radiation that may be due to both natural phenomena and nuclear detonations. The satellite must be designed to operate for a reasonable lifetime in the natural space environment. This environment is a function of orbital altitude. When the satellite is operating in midaltitude orbits, exposure to the earth's Van Allen belts will be predictable and its effect on radar electronics will be functions of the inherent hardness level of the components and the shielding used. (Reference 34 provides the trapped radiation data for proton and electron flux that has been measured as a function of altitude.) Figure 22.7³² shows the total 5-year dose in rads (Si) that satellites in orbits between 350- and 6500-nmi altitudes will experience as a function of the aluminum shielding used. It appears that current technology in integrated-circuit hardening should produce a total dose hardness of about $5(10)^5$ rads (Si) for devices that are suitable for the SBR T/R modules. This hardness level is adequate for SBR deployment in many of the candidate orbits with a mission life in the natural environment of several years. A hardness of $5(10)^6$ rads (Si) which may be achievable is required for a 5-year mission life. Survival in a saturated nuclear environment typical of a high-altitude nuclear burst requires a hardness of 1 to $5(10)^7$ rads (Si), depending upon the specific orbit. The development and consistent fabrication of devices as hard as this are relatively uncertain.

Tradeoffs. Obviously many tradeoffs can be made during the design of each type of SBR, depending upon the mission. In a dual-frequency surveillance and track radar performing an air traffic control (ATC) mission, as mentioned in Sec. 22.6, it is possible to trade off the length of the surveillance fence against the number of targets in track as functions of the track data rate and the radar-beam grazing angle. In a high-resolution-mapping radar mission it is possible to trade off the resolution against the orbital altitude as functions of radar wavelength and integration time. These trades are shown in detail in Refs. 12 and 13.

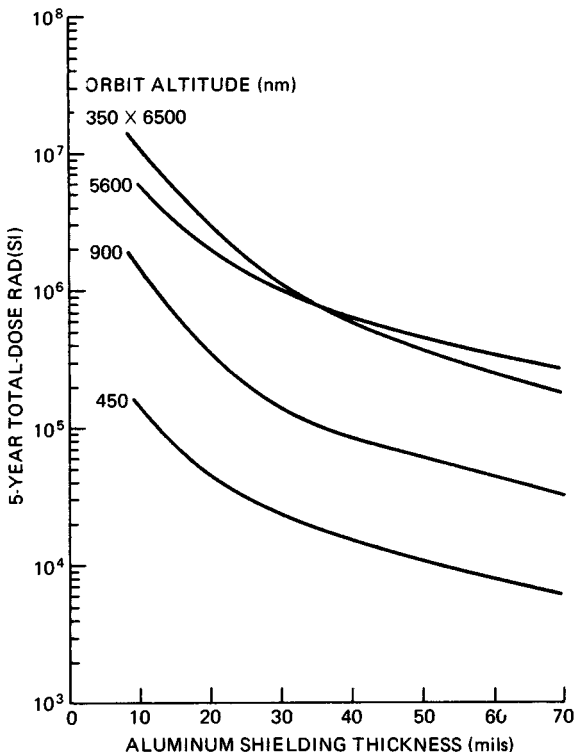


FIG. 22.7 Total dose versus shielding thickness for a 5-year mission.³²

Clutter/Interference. SBR performance is significantly dependent upon clutter and interference, either intentional or unintentional. To illustrate the magnitude of the clutter problem, consider the ATC radar described in Sec. 22.6. When the grazing angle is 70° and the reflectivity of the ground is -15 dB, the main-beam clutter cross section is $+57$ dBsm. If the desired radar performance requires that a target with an RCS of $+13$ dBsm have an SCR of 25 dB, then the main-beam clutter cancellation ratio must be at least 69 dB. Therefore, SBR performance requires large clutter cancellation ratios. Reference 35 indicates that clutter cancellation ratios up to 90 dB can be obtained by using pulse doppler and displaced phase center antenna (DPCA) techniques.

Interference will enter the SBR antenna primarily through the sidelobes since the beamwidth is narrow. This interference can be either intentional noise jamming or unintentional from other radars. These effects can be reduced to acceptable levels if adaptive sidelobe cancellation techniques and sidelobe-blanking techniques are utilized.

Launcher Capabilities. The most probable launch vehicle for the SBR is the STS (shuttle). Therefore, STS capabilities to put various payloads that include one or more SBR satellites (and the propulsion systems to place them into the desired orbits) must be considered. Figure 22.8 shows the STS cargo weight as a function of orbit inclination angle for various circular orbital altitudes and orbital-

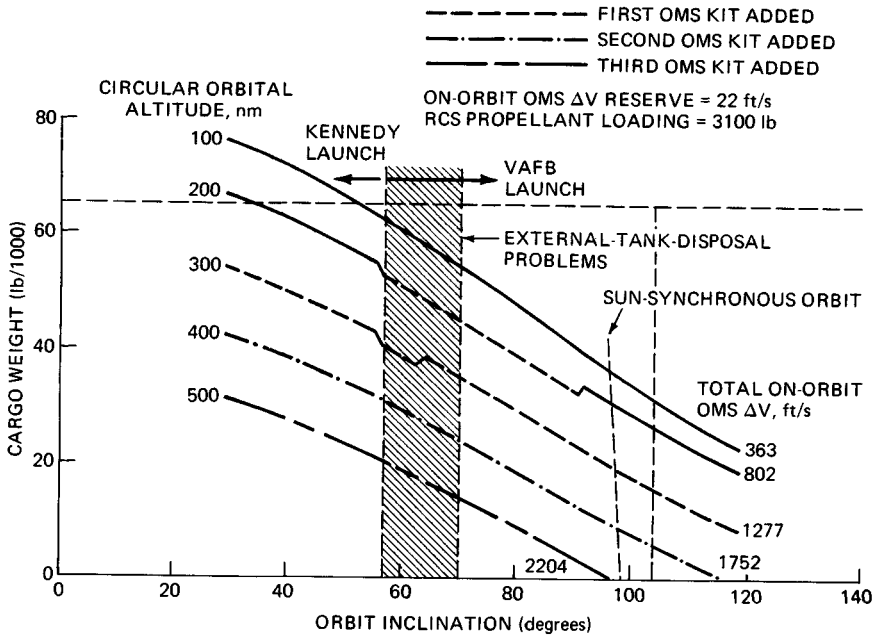


FIG. 22.8 STS (Shuttle) cargo weight versus inclination for various circular-orbit altitudes (delivery only—no rendezvous).

maneuvering-system (OMS) on-orbit velocity increments. It is seen that 64,000 lb can be delivered to a 100-nmi circular orbit inclined 50° from the Kennedy launch site in Florida. If each SBR weighs 9500 lb, then three SBR satellites can be placed into orbit along with 35,500 lb in propulsion for orbital transfer.

Advantages and Disadvantages of SBR Systems. When sensors are required for missions involving targets in space, ocean, and air and for missile defense missions, the use of SBRs should be considered. The advantages of such radars deployed in space compared with ground-based radars are described below.

1. Coverage in both space and time is limited only by the orbit selected and the number of satellites. Large-scale continuous observation can be obtained as shown in Figs. 22.9 and 22.10.²⁸ In Fig. 22.9 the required number of vehicles are shown as well as the number of orbit planes in which they are distributed to provide continuous coverage of the entire earth's surface from circular polar orbits. It is seen that six vehicles in two orbit planes can be used for vehicle altitudes greater than about 6000 nmi. There is no nadir hole in the satellite coverage. Figure 22.10 illustrates the special case of equatorial orbits and the number of vehicles required for continuous coverage. This situation is limited to the use of wide swaths that extend up to the specific latitudes indicated. It is seen that four vehicles can cover a 60° swath when the vehicles are at altitudes greater than about 6000 nmi. Temporal coverage is illustrated in Fig. 22.11, which shows the maximum time for viewing ground objects from a space vehicle if the objects are tracked.²⁸ It can be seen that a ground object can be observed for more than 7000 s when the orbital altitude is 6000 nmi.

2. When the SBR uses an electronic scanning antenna, it is possible to per-

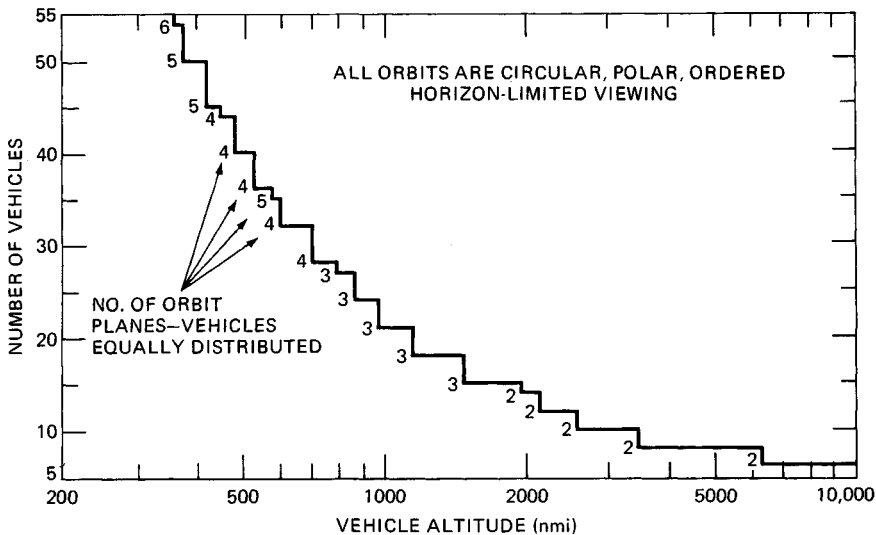


FIG. 22.9 Global coverage by polar orbits.²⁸

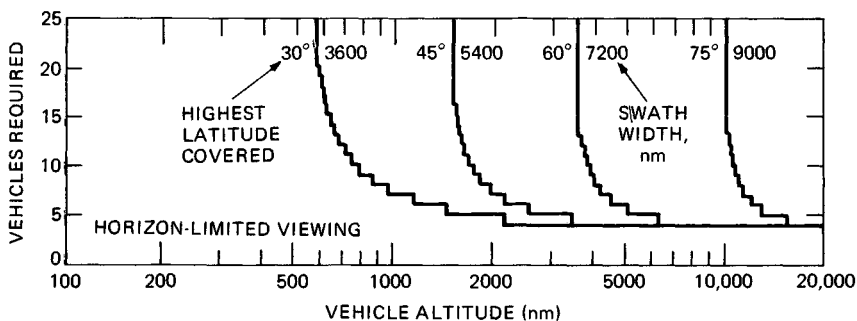


FIG. 22.10 Zonal coverage by equatorial orbits.²⁸

form multiple missions. For example, a system of radar satellites can (a) search a fence formed completely around the continental United States (CONUS) to detect bombers at a distance from the coast, (b) search a fence over the poles to detect intercontinental ballistic missiles (ICBMs) before they can be detected by the Ballistic Missile Early Warning System (BMEWS), (c) monitor potential launch sites for space launches from any foreign country, (d) perform surveillance of ocean areas, (e) search a sea-launched ballistic missile (SLBM) detection fence, and (f) detect objects in space that appear to be threats to United States synchronous satellites. The number of missions is limited only by the weight and prime power available, but even these limitations can be overcome when the space shuttle is the planned launch vehicle. Therefore, the only real limitations are technology and cost.

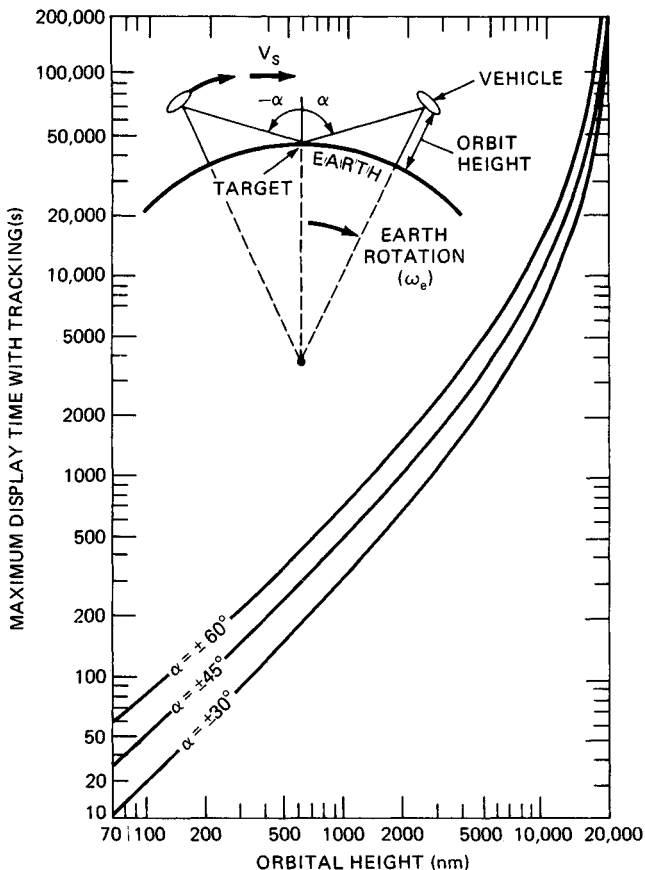


FIG. 22.11 Maximum time for viewing objects from a space vehicle if the objects are tracked.²⁸

3. Atmospheric propagation problems can be minimized by proper selection of operating frequencies and favorable geometry selection.

4. No overseas stations are required if data is read out via relay satellites. Hence, the SBR system allows a country to be politically independent, and the loss of tracking stations in a foreign country has no impact on its system capabilities.

The factors that affect the pace of development of large radar systems in space are:

1. The technologies of large antenna structures in space, of large phased arrays in space, of large weights in space, and of large prime power systems in space are considered to be in their early stages.

2. The funds that can reasonably be spent on a space-based multimission ra-

dar system are to be determined. Even with the use of the Shuttle to reduce the cost per pound of payload into orbit, large investment costs are expected to be required for the SBR system.

22.3 SBR SYSTEM DESCRIPTIONS

The United States and the U.S.S.R. have deployed Type I and Type II space-based radars. This section describes some of these SBR systems.

STS Rendezvous Radar.^{1,15,36} The Integrated Radar and Communications Subsystem (IRACS) was developed by Hughes Aircraft Company for use on the Space Transportation Systems (STS). The IRACS is a coherent range-gated pulsed doppler radar which searches for, acquires, and tracks other orbiting objects and provides the spatial measurement data needed to perform rapid and efficient rendezvous with those objects.

The IRACS performs both radar and communications functions for the STS. In the pulsed doppler radar mode it performs the rendezvous function just described. In the communications mode it searches for, acquires, and tracks the Tracking and Data Relay Satellite System (TDRSS) relay satellites to provide two-way communication between the space shuttle and ground tracking stations.

The IRACS hardware is subdivided into *deployed* and *inboard* assemblies. The deployed hardware is located within the Shuttle payload bay and is extended for operation through the open payload bay doors. Included in this hardware are the antenna reflector, feed, gimbals, drive motors, gyros, digital shaft encoders, rotary joints, transmitter, receiver, upconverter, first downconverter, and frequency synthesizer. The inboard hardware is located internally to the shuttle and includes the signal-processing, track-filtering, and control functions.

The K_u -band IRACS operates in the band of frequencies between 13.75 and 15.15 GHz, with radar operation between 13.75 and 14.0 GHz. There are two basic radar modes: a passive mode in which the target is noncooperative, in that no cross-section augmentation is present, and an active mode in which the target has an on-board transponder. The radar operates out to 12 nmi in the passive mode and out to 300 nmi, with a +14 dBm transponder, in the active mode. Submodes include an automatic search and angle and range track capability and external angle control operation. Under external angle control the antenna either is positioned by external slew commands or is referenced to inertial space or to the Shuttle axes. During automatic operation, angle, angle rate, range, and range rate measurements are made by the radar after track has been initiated. Under external angle control only range and range rate are measured.

The antenna is a 36-in-diameter center-fed parabola with 38.4 dB gain and 1.68° beamwidth. The five-element monopulse feed provides a sum and two orthogonal difference outputs. The difference outputs are time-multiplexed together into a *single* receiver difference channel for the angle-tracking operation. An auxiliary horn is monitored in the search mode, using the receiver difference channel, and compared with the main-antenna sum channel to prevent acquisition of large targets in the sidelobes of the main antenna. The auxiliary antenna has a peak gain which is about 20 dB less than that of the main antenna. Low-noise radio-frequency (RF) preamplifiers are used in the sum and difference channels. After amplification, at intermediate frequency (IF), the sum and difference channels are combined into a single receive channel for routing to the inboard elec-

tronics assemblies for further processing. The transmitter employs a traveling-wave tube (TWT) with 44 dB gain to amplify the coherent synthesizer output to 50 W of peak power. For short-range operation (down to 100 ft) the TWT is bypassed to reduce the power on the target. Five RF frequencies are used in the radar mode to decorrelate Swerling 1 (slowly fluctuating) target returns and improve detection. A 16-point digital Fourier transform (DFT) processor is employed to coherently integrate multiple pulse returns and to provide fine-resolution measurements of target relative velocity. The deployed assemblies weighed 135 lb, and the prime power was 460 W.

Seasat-A Synthetic Aperture Radar.^{18,37} The Seasat-A was a focused SAR consisting of five subsystems: (1) spacecraft radar antenna, (2) spacecraft radar sensor, (3) spacecraft-to-ground data link, (4) ground data recorder and formatter, and (5) ground data processor. The antenna was a microstrip array of eight panels that were fed by a corporate-feed network and operated at 1275 MHz. Details of the Seasat-A antenna are discussed in Sec. 22.4. The solid-state radar transmitter generated a nominal peak power of 800 W with a linear frequency modulation (LFM) derived from a stable local oscillator (stalo). The antenna illuminated a 100-km-swath width at the surface of the earth with an antenna elevation beamwidth of 6° that was oriented at an angle of 20° with respect to the nadir. Upon reception of the reflected signal by the receiver in the radar sensor, the return signal was amplified by a sensitivity-time-controlled RF amplifier. This signal and a fraction of the radar stalo were then combined and transmitted to a ground station by an analog data link. At the ground station, the data line demodulator recovered the radar sensor stalo and the radar return signal. The recovered synchronously demodulated video radar signal was then converted into digital form by the radar data recorder and formatter subsystem. Upon conversion, the signal was buffered and recorded by a high-density magnetic tape recorder. Subsequently, the radar data processor converted the digital recorded data into a two-dimensional map of the radar cross section of the area observed by the antenna. The SAR system generated a 25-m-resolution radar map in elevation (across track) by time-gated compressed radar return signals and in azimuth (along track) by focusing the coherent radar returns during the data-processing interval in the earth-based signal processor. Total SAR on-orbit weight was 223 kg; required radar prime power was 624 W. Table 22.3 gives the characteristics of the Seasat SAR.

Shuttle Imaging Radar.³⁶ The technology developed for the Seasat-A SAR formed the basis for the shuttle imaging radar (SIR) series, SIR-A and SIR-B. Minor differences in the antenna will be discussed in Sec. 22.4. The L-band radar transmitter was utilized with slight bandwidth changes so that resolution was 40 m on SIR-A and 20 m on SIR-B. Swath width was 50 km for both radars. Orbital altitudes were 240 km and 220 km, respectively, so that radar range and incidence angles were different.

GEOS-C SBR System Characteristics.^{8,19-21} The GEOS-C radar altimeter was a precision K_u -band (13.9-GHz) SBR altimeter developed primarily to measure ocean surface topography and sea state. It was a complex multimode radar system with two distinct radar gathering modes (global and intensive modes) and two corresponding self-test-calibration modes for use in on-orbit functional test and instrument calibration. The key performance features were its capability to (1) provide precise satellite-to-ocean surface-height measurements [precision

TABLE 22.3 Synthetic Aperture Radar

Antenna	
Type	Planar phased array (10.74 m × 2.16 m)
Beamwidth	1.1° azimuth, 6° elevation (1 dB points)
Look angle	20° depression, 90° with respect to the velocity vector
Gain	34.7 dB
Polarization	Horizontal
Weight	113 kg
Transmitter	
Type	Solid-state transistor
Efficiency	38 percent
RF carrier	1275 MHz
Peak power	800 W (nominal), 1125 W (maximum)
Pulse length	33.8 μs
PRF	1463, 1540, 1645 pps
Duty cycle	0.05 (maximum)
Average power	44.5 W (nominal), 62.6 W (maximum)
Waveform	Pulse, LFM, 19-MHz Bandwidth
Receiver	
Noise temperature	550 K
Bandwidth	22 MHz
System input noise	-127.42 dBW
AGC time constant	5 s
STC gain variation	9 dB
Stalo stability	3×10^{-10} in 5 ms
Recorder	25 kb/s digital
System weight	110 kg (excluding antenna)
Total prime power	624 W (maximum)
Resolution	25 m
Swath width	100 km
Swath length	2000 km per pass
Swath orientation	Right side of orbit path
Signal-to-noise ratio	9 dB (nominal)

of 50 cm in the global mode (GM) and 20 cm in the intensive mode (IM) at an output rate of one per second] for use in mapping the shape of the ocean surface and (2) provide data which can be processed to estimate peak-to-trough ocean waveheight (waveheights in the range of 2 to 10 m can be estimated to an accuracy of 25 percent). Several key areas of technology included in the design are (1) high-frequency logic circuitry with a 160-MHz clock and four-phase division for 1.56-ns resolution, (2) a wideband (100-MHz) linear FM pulse compression system with a compression ratio of 100:1 and a compressed pulse width of 12.5 ns, (3) high-speed sample-and-hold circuitry for accurate sampling of wideband (50-MHz) noisy video return signals, and (4) design and packaging of high-voltage (12-kV) power supplies for space application.

The instrument weighs 68 kg (150 lb) and occupies a volume of 0.119 m³ (4.2 ft³) including the antenna, which is a 0.6-m (24-in) diameter parabolic dish with

a 2.6° beamwidth and a 36 dB gain. The instrument is packaged in two basic sections: an RF section and an attached electronics section, which are both mounted to a center-cylindrical disk baseplate with a diameter of 0.65 m (26 in). The major subsystems contained in the RF section are (1) the IM transmitter (chirp generator, upconverter, 1-W driver TWT and high-voltage power supply, 2-kW output TWT and high-voltage power supply), (2) the GM transmitter (a 2-kW peak-power magnetron and high-voltage power supply), (3) the RF switch assembly (RF switches, waveguide runs, calibrate attenuation path, and TR switch), and (4) the receiver front end (downconverter-preamplifier). The major subsystems contained in the attached electronics section are (1) the IF receiver (IF amplifiers, filters, pulse compressor, detectors), (2) the signal processor (AGC, acquisition, and tracking functions implemented with analog and digital circuitry on multilayer board assemblies), (3) the frequency synthesizer, (4) the mode control circuitry, (5) the calibrate-test circuitry, and (6) the low-voltage power supply. The nominal power required for operation was 71 W for the global mode and 126 W for the intensive mode (16 waveform samplers).

U.S.S.R. Cosmos 1500 Side-Looking Radar.^{38,39} The U.S.S.R. launched the Cosmos 1500 oceanographic satellite on Sept. 28, 1983, into a nominal 650-km polar orbit. The satellite was the first of a series intended to provide continuous world ocean observations for civil and military missions. The sensors provide side-looking radar (SLR), radiometric, and visual coverage of oceans and ice zones for land- and sea-based users through an operational distribution network.³⁸ Table 22.4 summarizes the parameters and performance of the real-beam SLR. The radar operates at a frequency of 9500 MHz with a magnetron transmitter that has a peak power output of 100 kW. The antenna is a slotted waveguide that is 11 m long and 4 cm high. Cosmos 1500 has demonstrated many significant capabilities, including (1) routine automatic picture transmission of SLR images of earth; (2) mapping of inhomogeneities of Antarctic and Greenland ice cover that were previously not detected; (3) radar images of polar regions of multiyear and first-year ice zones; (4) mapping of elongated zones of ice-cover continuity disturbances; (5) tracking of sea-ice drift by using a series of radar images of the same water area; (6) detection of oil slicks, wind fields, and currents; and (7) guidance of ships trapped in arctic ice during October–November 1983.

The orbit of Cosmos 1500 allowed complete earth coverage each 1.41 days for the optical sensors and each 5.9 days for the radar sensor. Subsequent launches of the Cosmos 1500 type of satellite have occurred.

22.4 TECHNOLOGY

The desire to develop large radars in space has stimulated progress in several new technologies such as (1) large deployable parabolic and phased array antennas, (2) lightweight, low-cost monolithic microwave integrated circuit (MMIC) transmit/receive modules, (3) high-level prime power systems, (4) efficient on-board signal processors, (5) large lightweight space structures, (6) lightweight, low-cost phase shifters, (7) radiation-hardened electronic devices, (8) materials with a low thermal coefficient of expansion, and (9) advanced calibration and self-test techniques. Some of these technologies are briefly reviewed here.

TABLE 22.4 Cosmos 1500 SBR Parameters and Performance

Type	Real-beam side-looking radar (460-km swath)
Frequency/wavelength	9500 MHz/3.15 cm
Antenna	
Type	Slotted waveguide
Size	11.085 m × 40 mm
No. of slots	480
Illumination	Cosine on a pedestal
Beamwidth	0.20° × 42°
Gain	35 dB
Sidelobes	-22 dB to -25 dB
Waveguide	Copper, 23 × 10-mm cross section
Polarization	Vertical
Swing angle	35° from nadir
Noise temperature	300 K
Transmitter	
Type	Magnetron
Power	100 kW peak, 30 W average
Pulse width	3 μs
PRF	100 pps
Loss	1.7 dB
Receiver	
Type	Superheterodyne
Noise power	-140 dBW
Loss	1.7 dB
Pulses integrated	8 noncoherent
LNA noise temperature	150 to 200 K
LNA gain	15 dB
Dynamic range	30 dB
IF	30 MHz ± 0.1 MHz
Input power	400 W
Range	700 km (minimum), 986 km (maximum)
SNR	0 dB on $\sigma^0 = -20$ dB

Antennas. The development of SBR is strongly dependent upon the technology of large space-deployable antennas. Large antennas must be used since the radar ranges are significantly greater than usual and the prime power in the radar is limited. The vacuum of space and the zero-g environment permit the deployment of antennas with low mass per unit antenna area. Antennas with large diameters, up to 1 km, have been discussed by United States developers.⁴⁰⁻⁴⁸ In the U.S.S.R., antennas with diameters in the 1- to 10-km range have been discussed.⁴⁹ In addition to being large and deployable, the SBR antenna must maintain its desired shape whether it be parabolic or planar. As shown earlier (Fig. 22.3), small deviations can cause a significant loss in antenna gain. Stable configurations are obtained by using low-coefficient-of-thermal-expansion (CTE) materials. Characteristics of selected materials for stable RF systems are shown in Table 22.5. Data includes CTE, density, modulus, conductivity, and attenuation of WR 75 waveguide fabricated

TABLE 22.5 Potential Material Selection for Thermally Stable RF System

Material	Expansion coefficient, in/(in ³ °F) × 10 ⁻⁶	Density, lb/in ³	Young's modulus, × 10 ⁶ lb/in ²	Thermal conductivity, Btu · in / h · ft ² · °F	WR75 attenuation, dB/ft at 11.95 GHz
Aluminum	13.1	0.10	10	1513	0.049
Titanium	5.1	0.16	16	444	0.274
Invar	1.1	0.29	20	93	0.370
Beryllium	6.8	0.07	40-44	1138	0.082
Graphite/epoxy	0.03	0.06	17-25	75 (axial), 7.3 (transverse)	1.560 (bare), 0.040 (coated)
Gold	6.8	0.70	...	2064	0.048
Copper	7.8	0.32	...	2944	0.040
Silver	11.0	0.38	...	3101	0.039
Rhodium	4.7	0.45	...	611	0.087
Kevlar®* 49	- 1.1 longitudinal, + 33 radial	0.052	19	0.334 (axial), 0.285 (transverse)	

*®Du Pont trademark.

out of each material. In the following discussion selected antenna designs are described to illustrate the state of the art in large antennas in space.

United States Space-Deployable Antennas. A large space-deployable antenna that the United States deployed in space was the Lockheed-NASA ATS-6 parabolic reflector, launched in 1974. It was 9.1 m in diameter with a tolerance of 1.52 mm rms and a specific weight of 1.4 kg/m².^{41,50} The ATS-6 antenna embodies the flex-rib technique. During the years subsequent to that launch, Lockheed has evolved flex-rib deployment technology to additional reflector designs, the polyconic and the maypole designs.⁴¹

Harris developed the radial-rib double-mesh design and in 1970 built a 12.5-ft-diameter antenna.⁴⁰ This was followed by the TDRSS 4.88-m-diameter antenna and three generic antenna designs including the radial-rib, TRAC, and hoop-column concepts. The weight-versus-diameter capabilities of these three designs are shown in Fig. 22.12.⁴⁷ As part of the NASA deployable antenna flight experiment (DAFE) design study, Harris estimated that a 50-m-diameter reflector assembly would have an overall weight of 819 kg (1805 lb).

The specific mass of this design is 0.417 kg/m², and the estimated surface error was 4 mm rms. In a parallel DAFE competition, the Grumman Aerospace Corporation designed a 50-m-diameter phased array lens antenna that would have a specific mass of 0.522 kg/m².

The DAFE studies were conducted for NASA Marshall Space Flight Center (MSFC) by Harris and Grumman in a competition during the period from August 1980 to September 1981. The primary objectives of the study were (1) to demonstrate, by a flight experiment, the capability to launch, deploy, retract, and return to earth a large (50-m-diameter) space frame; and (2) to verify, by flight experiment, the capability of the space frame to attain and maintain the dimensional

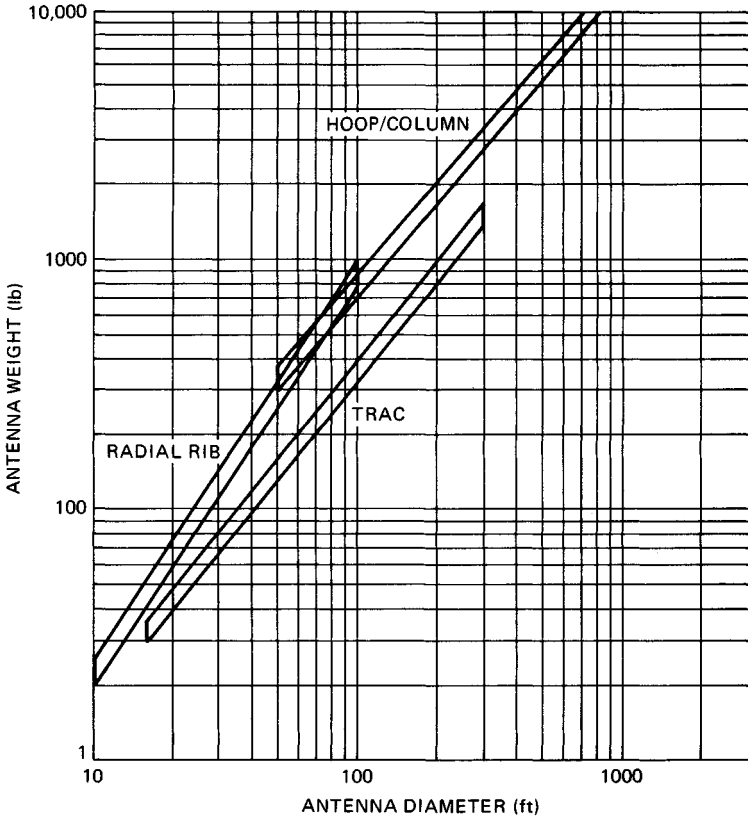


FIG. 22.12 Weight versus diameter for three generic antenna designs.⁴⁷

precision required to operate as a spaceborne antenna. Both contractors devised orbiter-attached experiments that would maximize program outputs while minimizing orbiter and experiment risks. Although many flight configurations were designed, overall results were similar for both phased array and parabolic antennas. Both contractors also devised measurement techniques that would provide a 50-mil rms accuracy required for the measurement of antenna deformation.

General Dynamics has designed space-erectable antennas and parabolic graphite-epoxy reflectors for space applications.^{43,46} A 2.44-m-diameter reflector was built and tested. It has a surface tolerance of 0.0635 mm rms and a specific mass of 4.4 kg/m². The space-erectable designs had a specific mass of 0.49 kg/m²; however, the tolerance was on the order of 10 mm rms. Therefore, the space-erectable antenna designs were configured primarily for relatively low-frequency operations.

TRW has developed an advanced antenna concept under work sponsored by JPL as part of the NASA large space systems technology (LSST) program.⁵¹ The feasibility of stowing large, solid antenna reflectors in the Shuttle was examined. The antennas would be designed to operate in the 10- to 100-GHz range and main-

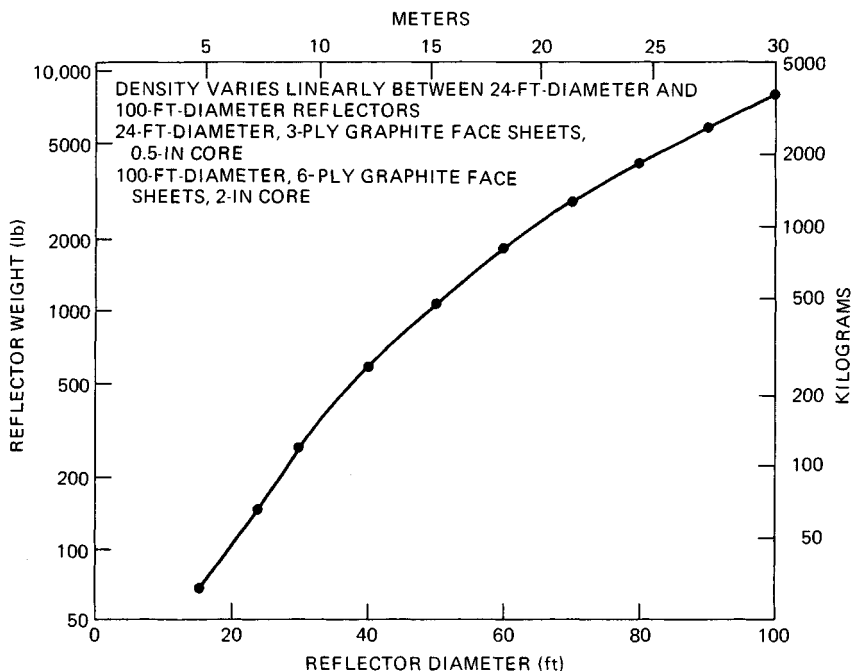


FIG. 22.13 TRW antenna reflector weight estimate.⁵¹

tain rms deviation on the order of 10^{-5} -diameter fabrication error. Thermal deviation for a 100-ft-diameter antenna was estimated to be 0.0034 in rms. The weight of antenna reflectors was estimated for diameters of 16 to 100 ft. Figure 22.13 shows the plot of reflector weight excluding the weight of feeds and subreflectors. The basic construction assumed a graphite-epoxy-aluminum honeycomb-sandwich configuration.

Antenna systems have been studied and fabricated under the LSST program. Lockheed Missiles and Space Company (LMSC) has demonstrated, in a simulated zero-gravity environment, the technology for a large space-deployable antenna.⁵² LMSC fabricated a 22.5° sector of a 55-m-diameter *wrap-rib* parabolic antenna and deployed it in a ground-based zero-*g* facility. The surface of the antenna is a knit mesh of 1.2-mil gold-plated molybdenum wire that is contoured by graphite-epoxy ribs. Each rib weighs 9.1 kg, is 27.5 m long, and is lenticular in shape. This shape allows the ribs to collapse as they are wrapped around a central hub for stowage prior to deployment. The ribs resume their required structural shape as they unwind (under constraint), thereby stretching the mesh into the proper parabolic shape. The Lockheed development program was initiated to demonstrate the readiness of large-diameter offset reflector technology through development of ground-testable, flight-representative full-size hardware.

The Seasat-A antenna (designed by Ball) is a 10.74- by 2.16-m microstrip array that is deployed after orbit insertion. The operating wavelength is 23.5 cm. This antenna is very similar to the SIR-A. Both are significant developments in large deployable antennas.^{6,37} The SIR-B antenna is similar except that it was mechan-

TABLE 22.6 Characteristics of Seasat, SIR-A, SIR-B, and SIR-C Antennas

	Seasat	SIR-A	SIR-B	SIR-C
Frequency	1275 MHz	1278 MHz	1282 MHz	1275 and 5300 MHz
Bandwidth (1.5:1 VSWR)	22 MHz	8 MHz	16 MHz	> 20 MHz
Gain	34.9 dB	33.6 dB	33.0 dB	37.0 dB (L band); 43.0 dB (C band)
Polarization	Horizontal linear	Horizontal linear	Horizontal linear	Horizontal linear and vertical linear
Beamwidths <i>H</i> plane	6.2°	6.2°	6.2°	Adjustable through amplitude and phase, 0.99° L band; 0.24° C band
<i>E</i> plane	1.1°	1.4°	1.1°	
Beam-pointing angle	20.5°	47°	15 to 60° (mechanical steering)	Tilted to 35°, then ±25° electronically steered
Size (deployed)	10.74 × 2.16 m	9.4 × 2.16 m	10.74 × 2.16 m	12.06 × 4.2 m
Size (folded)	1.34 × 2.16 m		4.1 × 2.16 m	4.1 × 4.2 m
Weight	103 kg	181 kg	306 kg	900 kg
Support structure	Graphite-epoxy 3D truss	Rigid aluminum 3D truss	Rigid aluminum 2D and 3D truss	Graphite-epoxy 2D truss
Fold mechanisms	Multifold (spring-loaded)	Fixed	Two folds (motor-driven)	Two folds (motor-driven)
Number of radiating elements	1024	896	1024	864 (L band); 5184 (C band)
Number of panels	8	7	8	9
Feed system	Microstrip, coaxial and suspended substrate	Microstrip, coaxial	Microstrip, coaxial	Microstrip, coaxial, waveguide
<i>W/A</i> , kg/m ²	4.44	8.9145	13.1906	17.7683

ically steerable. The SIR-C antenna is electronically steerable and dual-frequency. Table 22.6 summarizes the RF and mechanical characteristics of the Ball Seasat-class antennas.

Ball Aerospace Systems Division designed an antenna for the low-altitude space-based radar (LASBR) mission.⁵³ The 13.8- by 63.6-m array is a direct extension of space-proven Seasat and SIR-A technology with stringent constraints of array two-way sidelobe and beam skirt performance. The design features a single-axis deployable truss fabricated from graphite-epoxy microstrip honeycomb panels and passive 3-bit hybrid phase shifters at each of the 49,152 elements. The loss and weight penalty ($W/A = 4.02 \text{ kg/m}^2$) of a corporate-feed network is compensated for by using transmit and receive gain at each of 384 subpanels.

U.S.S.R. Cosmos 1500 Antenna. On Sept. 28, 1983, the U.S.S.R. launched the Cosmos 1500 satellite with an SLR for the all-weather probing of the surface and ice cover of the earth's seas and oceans.³⁸ (The SLR was mentioned in Sec. 22.3.) The antenna is a slotted-waveguide array of 480 slots with a length of 11.085 m and a height of 4 cm. The operational wavelength is 3.15 cm. The beamwidth of the antenna is 0.2 by 42° , providing a gain of 35 dB. The antenna is constructed out of a copper waveguide that measures 23 by 10 mm in cross section. The slots are in the wide wall, with variable spacing to provide a cosine on a pedestal amplitude distribution. Figure 22.14 shows the antenna during deployment. The five sections of the antenna are mated and held in position by spring-loaded locks on the ends that are operated by release mechanisms at the end of the deployment cycle. Helical springs are provided on the flange faces along the wide wall for electrically tight joints. Relative leakage power between sections is down by 50 dB. After deployment, the antenna can be rotated through 35° from the nadir.

Transmit/Receive Modules. During the advanced development stage of large phased array space-based radars, the use of small, low-cost, lightweight low-power T/R modules was proposed in active array configurations.⁵⁴ Goals for these T/R modules³¹ included costs of less than \$100 each in large mass production and a size of 1 in^2 , using 0.5 to 1 W of power. Each module contains a phase shifter, drivers, logic switches, power amplifiers, low-noise receiver, and other components. They can also include a means for sensing and compensation of element displacement error. Further information on solid-state transmitters and transceiver module characteristics is found in Chap. 5.

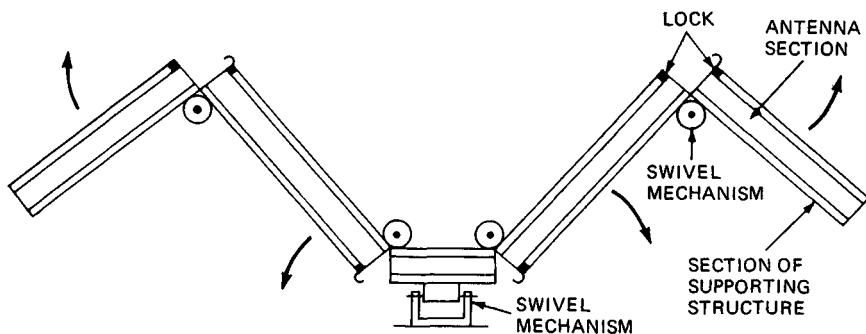


FIG. 22.14 Schematic of the antenna module for Cosmos 1500.

On-Board Processors. The bandwidth requirements for the satellite communications data link can be reduced when an on-board processor is utilized. The major functions of an on-board processor in a large SBR can include pulse compression, doppler filtering, adaptive beamforming, calibration, range walk correction, video integration, constant false-alarm rate (CFAR), monopulse error signal, burst waveform weighting, sidelobe blanking, and editing out interference.

In addition to providing these functions, the processor must be low-powered, have low mass, operate for many years without manual repair, and have radiation-hardened memories. Technology using 16K random-access-memory (RAM) chips and very-large-scale-integration (VLSI) computers can reduce "typical" system power and mass from 3 kW and 2000 lb, respectively, to 400 W and 400 lb.⁵⁵ The Defense Advanced Research Projects Agency (DARPA) and others have been working on the development of an advanced on-board signal processor (AOSP) and have made considerable progress.¹⁰ The concern here is to develop a very reliable and survivable on-board computer using gallium arsenide circuitry that can resist the electromagnetic pulse and other radiation effects produced by nuclear detonations. AOSP program technical goals include (1) prime power of 100 W, (2) weight of 100 lb, (3) volume of 2 ft³, (4) 5-year life with a probability of survival of 95 percent, and (5) an input rate of 50 million words per second.^{32,56}

Prime Power. The performance of any SBR will ultimately be limited by the prime power system. The most frequently utilized source of prime power for satellites is the solar-battery configuration. High-efficiency GaAs solar cells have demonstrated efficiencies of 18 percent.⁵⁷ With the addition of other subsystems, including panels, rotary joints, slip rings, battery, power control, and distribution equipment, the specific power density of the prime power system is on the order of 13 to 24 W/kg. Solar-battery systems are limited and have several disadvantages that will be discussed later.

Space nuclear prime power systems offer certain advantages to SBR, and they have been launched into space by the United States since 1961, beginning with the SNAP-3A. Of the nuclear power systems that were placed into orbit between 1961 and 1977, only one was a nuclear reactor, SNAP-10A. Since then the technology has advanced⁵⁸⁻⁶¹ to the extent that it is estimated that an SP-100 type of nuclear reactor would have a mass of 2770 kg and a power output of 100 kW, thereby providing a specific power density of 36 W/kg.

Two baseline deployment configurations of solar-battery and nuclear prime power systems were designed with two power levels, 25 and 100 kW, for the same deployment altitude and are shown in Fig. 22.15.⁶¹ It is seen that the solar systems are larger than the nuclear. As the power level increases, the increased size of the solar system becomes more pronounced. In comparing overall lengths, the 100-kW solar system is 2.4 times the length of the nuclear system. The weight of the solar system depends upon the orbital altitude and the operational requirement during eclipse. For a continuous-operation solar array at geosynchronous altitude, the 100-kW solar system weight is estimated to be 3970 kg.

In comparing advantages and disadvantages, the solar-battery system is based on known technology, and extrapolation to a larger power output is considered to be an engineering design task. The nuclear reactor design re-

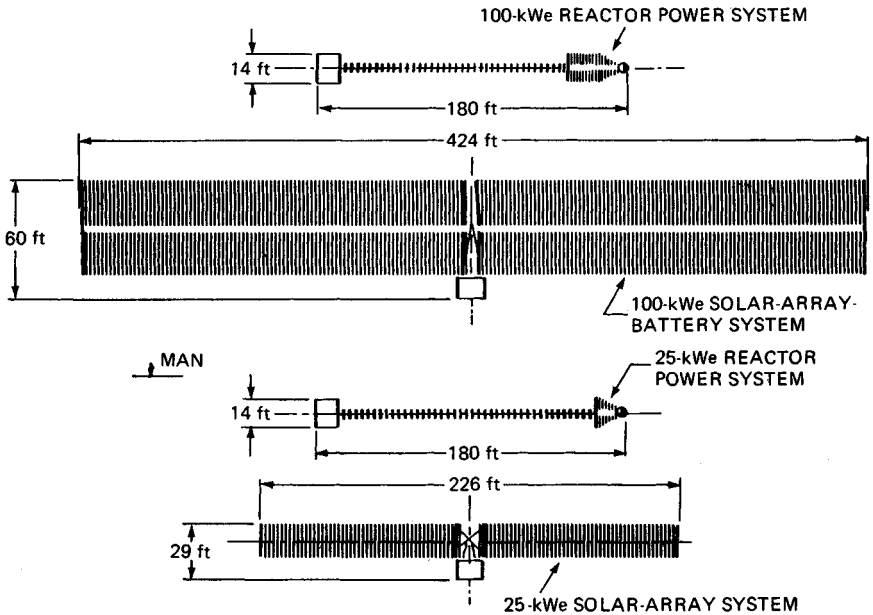


FIG. 22.15 Baseline prime power systems: deployed configurations.⁶¹

quires engineering development. The advantages of nuclear prime power systems include (1) reduced mass and size at the higher power levels; (2) no perturbation by natural background in low earth orbit (LEO) and geosynchronous orbit (GEO); (3) no need for alignment, gimbaling, slip rings, and long-life batteries, suggesting that the nuclear system will have significantly enhanced reliability; (4) reduced effect on SBR antenna, i.e., multipath and sidelobes; (5) nuclear-hard compared with solar systems; (6) reduced optical and radar signature; (7) reduced cost by a factor of 3; (8) continuous availability of power; (9) no orientation requirements; (10) no maneuver limitations; (11) no power degradation, i.e., beginning-of-life–end-of-life (BOL-EOL) power level; and (12) no large, flexible structure.

The issue of safety was addressed in 1980 by the United Nations Working Group report,⁵⁹ which studied the safety of nuclear power sources (NPS) in space. That group reaffirmed the conclusion that NPS can be used safely in space. It placed responsibility on the launching nation to (1) conduct safety tests and evaluations consistent with international standards; (2) provide the United Nations with detailed design and test data of the NPS at launch time; and (3) when reentry of the NPS becomes reasonably certain, provide the United Nations with details of orbiting parameters, probable impact regions, power history, inventory of nuclear fuel, and radiation dosage at 1 m for survival sections. The working group noted that U-235-fueled reactors required 400 years' decay time to reduce fission product activity by a factor of 1000. It implied that a minimum orbit altitude of 300 nmi should be used.

It is obvious from a technical point of view that nuclear prime power systems should be utilized for large SBR systems whenever high power is required.

22.5 CRITICAL ISSUES

A succinct treatment of selected critical issues is given here. The critical issues in the development of SBR include (1) system cost, (2) system survivability or vulnerability, (3) system calibration, (4) antenna deployment and distortion, (5) on-board processing, and (6) nuclear prime power.

SBR System Costs. The author uses a cost-estimating ratio for SBR satellites of \$64,000 per kilogram in 1988 dollars that is based upon informal study of many satellites that have been placed into orbit. Launch costs are not included; they depend upon the launch vehicle. Informal study of many satellite launches has resulted in the data shown in Fig. 22.16, which gives a launch cost for several types of vehicles when launched from two United States launch sites, the Eastern Test Range (ETR) and the Western Test Range (WTR). It can be seen that polar orbit costs are greater than launches from the ETR due east and that it is more economical (on a dollars-per-pound basis) to launch large payloads on STS and Titan class vehicles.

Survivability and Vulnerability. SBR system survivability and vulnerability must be demonstrated and tested. The natural space radiation environment will cause a significant total dose on a T/R module depending upon its shielding. Table 22.7 is a summary of the total dose for a 5-year period for circular orbits at altitudes of 450, 900, and 5600 nmi.³² The T/R module in the analysis has an area of 1 in², and it has been assumed that the total dose values will be double those expected in order to account for the particle radiation that penetrates both sides of the module package. Some shielding may be provided by the chip substrate; however, this has been ignored.

22.6 SBR FUTURE POSSIBILITIES

Rendezvous Radar Missions. All satellite rendezvous missions have been performed by manned vehicles. In the foreseeable future, the majority of rendezvous missions might be conducted by unmanned vehicles such as the OMV. The planned list of missions for the OMV includes (1) large-observatory servicing at the shuttle, (2) payload placement, (3) payload retrieval, (4) payload reboost, (5) payload deboost to reentry, (6) payload viewing, (7) subsatellite mission, (8) multiple-payload mission, (9) in situ servicing mission, (10) STS transfer to space station, and (11) base support. Details of these missions may be found in the NASA OMV request for proposal.⁶² The initial design of the OMV is modular so as to permit upgrading its capability to operate from the space station and to accommodate the following growth missions by the addition of appropriate kits or elements to the system: (1) logistic support, (2) debris collection mission, (3) extended on-orbit operation, (4) satellite buildup, (5) satellite refueling, (6) servicing mission, and (7) space station reboost.

A rendezvous radar that is low in cost and light in weight will be used to perform these future OMV missions. Such an OMV radar might have the major performance characteristics shown in Table 22.8. The rendezvous radar set (RRS) will be an X-band coherent, range-gated, pulse doppler radar with redundant

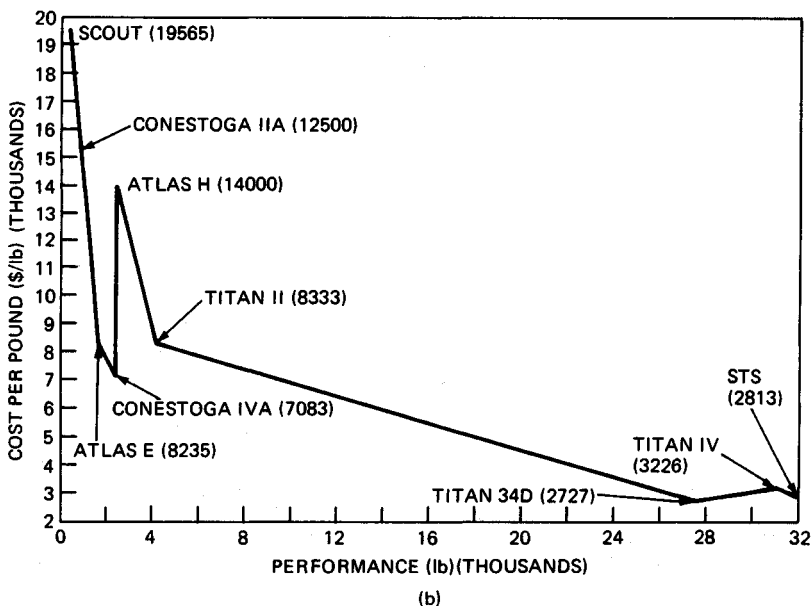
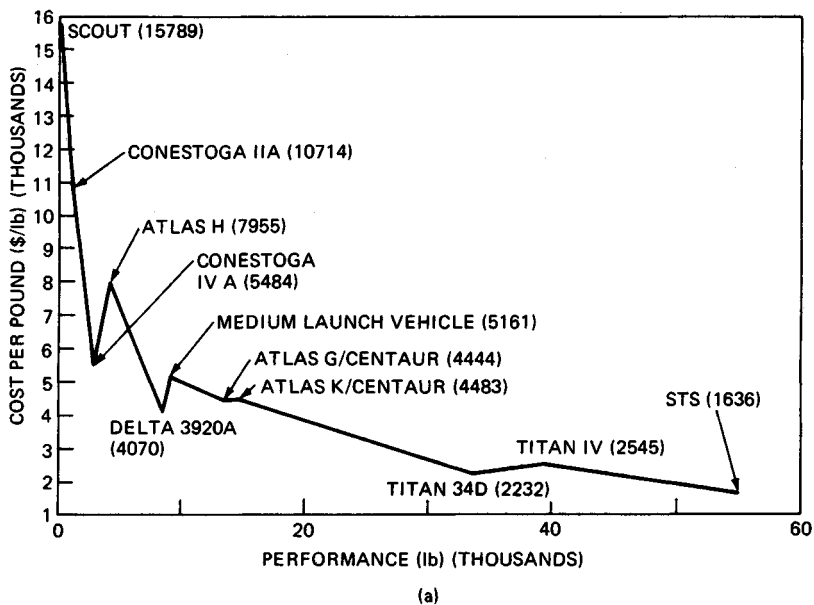


FIG. 22.16 Cost per pound to low earth orbit. (a) Eastern Test Range launch due east. (b) Western Test Range launch into polar orbit.

TABLE 22.7 Space Radiation Environment Summary*

SBR orbit, nmi	5-year total dose, rads (Si); aluminum shielding thickness		
	15 mils	25 mils	50 mils
450	2(10) ⁵	6(10) ⁴	2(10) ⁴
900	2(10) ⁶	4(10) ⁵	2(10) ⁵
5600	6(10) ⁶	4(10) ⁶	(10) ⁶

*From Ref. 32.

TABLE 22.8 OMV Radar Characteristics

Frequency	9.5 to 9.8 GHz
PRF	6.67 kHz
Pulse width	0.05, 0.2, 1.5, and 15 μ s
Transmitter peak power	2 W (GaAs FET with \approx 30-dB gain)
Receiver noise figure	< 4 dB, GaAs FET LNA
Antenna	Planar slotted array, linear polarization
Antenna size	14 by 15 by 1 in
Antenna gain and beamwidth	30.5 dB (at 9.65 GHz) and 5.0°
Search scan	\pm 20° cone, with 5-min scan time
Angle accuracy (3 σ)	20 mrad
Range accuracy (3 σ)	Greater of 20 ft or 2 percent of range
Range rate accuracy (3 σ)	Greater of 0.1 ft/s or 2 percent of range rate
Deployed assembly weight	26 lb
Inboard assembly weight	50 lb (redundant total)
Electronics volume	\approx 2 ft ³ (redundant total)
Prime power	< 60 W

electronics and redundant gimbal motor windings. The OMV system computer initiates the acquisition-search function to permit detection of a 1-m² Swerling 1 target at a 4.5-nmi range (with 99 percent probability of detection and a false-alarm rate of one alarm per hour.) Monopulse tracking is performed to within a minimum range of 35 ft. Peak power is programmed over a 50 dB range during the rendezvous maneuver to minimize the RF radiation intensity on sensitive targets. Pulse frequency agility is utilized; up to 30 carrier frequency changes in 10-MHz steps over the 300-MHz operating band are used to decorrelate Swerling 1 target fluctuations. At each dwell, 128 pulses are coherently integrated in the fast Fourier transform (FFT) processor prior to noncoherent integration of the FFT outputs. Up to 30 FFT outputs can be integrated.

Initial configuration of the Space Station will have limited tracking-system requirements that include tracking of cooperative vehicles within a 37-km control zone.⁶³ This is based upon the assumption that all vehicles will provide accurate position and velocity data to the space station tracking system by way of the space-to-space link. Automatic tracking of an extravehicular (EV) astronaut is not required. For growth configurations of the Space Station, the tracking system

must expand to meet additional requirements. More co-orbiting vehicles, noncooperative or disabled vehicles, automatic tracking of EV astronauts, and sensors for berthing and docking operations will require additional tracking capabilities within the system. Some type of short-range radar may be required to track vehicles which do not have global positioning system (GPS) capability or vehicles which have been disabled. Results of preliminary tradeoffs on multiple-target tracking radars indicate³⁶ that either a K_a -band or an X-band phased array radar would be the preferred approach.

Remote-Sensing Missions.⁶⁴ SBR will participate in many remote-sensing missions for observation of the earth and the planets. The SIR series is expected to have the capability to image the earth's surface by using all polarization states (*HH*, *VV*, and *HV*) and with multiple frequency bands.

A number of SBR SAR missions have been considered by various countries for various purposes. An example is the Canadian Radarsat, which employs a C-band SBR SAR primarily for monitoring polar ice dynamics for use in ship routing; the SAR will have a 200-km swath.

In planetary exploration areas, SBR imaging systems are key elements for the exploration of two bodies that are continuously cloud-covered, Venus and Titan. In the exploration of Venus during the late 1970s, a radar sensor on the Pioneer Venus Orbiter provided low-resolution (40 to 100 km) images of the planet. A U.S.S.R. Venera satellite⁶⁵ produced radar images of part of the northern hemisphere of Venus with a resolution of 1300 m. The United States Venus radar mission has the objective of providing global coverage with a resolution of 150 m. In the exploration of Titan, a satellite of Saturn, the larger distance to the earth will put a very tight limit on data rate transmission, which directly impacts mapping coverage and resolution. A radar can be placed into orbit around Saturn, and on selected orbits the spacecraft will fly by Titan. These flybys will be targeted so that during each flyby a different region of Titan will be mapped with an SBR SAR. The Titan radar mapper will have a very wide swath (600 to 800 km) to obtain a global map during the small number of flybys. Real aperture imaging will provide a resolution of 6 to 40 km. A synthetic aperture mode can be used to observe limited regions with a resolution of about 200 m.

Other missions using radar are planned for ocean scatterometry and altimeters. Scatterometers are used to obtain accurate measurement of global surface winds for oceanography and meteorology. Wind speed with errors of about 2 m/s and a wind direction error of less than 16° are sought. SBR altimeters expect to measure altitude with an error of 5 cm from a 1300-km polar orbit inclined 65° over the ocean. Over the solid surface of Mars, a 37-GHz altimeter on the Mars orbiter mission expects to gather global high-resolution topographic mapping data with a height resolution of 15 m.

The overall goal of the Earth Observing System (EOS) is to advance the scientific understanding of the entire earth system on the global scale through developing a deeper understanding of the components of that system, interactions among them, and how the system is changing.⁶⁶ International space station elements include the following satellites in polar and equatorial orbits (1) a NASA EOS platform at 824 km, sun-synchronous, 1:30 P.M. equator-crossing time, ascending-node orbit; (2) a European Space Agency (ESA) platform at 824 km, sun-synchronous, 10:00 A.M. equator-crossing time, descending-node orbit; and (3) the manned space station in a 335- to 460-km 28.5° inclined orbit. Instruments planned for the satellites include radar, radiometers, IR, optics, and ultraviolet (UV). These sensors will measure parameters such as winds, clouds, rain, liquid-moisture content, geologic parameters,

ocean currents, etc. Radars will be used to make atmospheric and geological observations. Two of the radars proposed are the tropical-rain mapping radar (TRAMAR) and the land, ocean, and rain radar altimeter (LORRA).⁶⁷

Global Air Traffic Surveillance.¹² ATC is increasingly a matter of global concern, and the explosive growth of aircraft density in, around, and between major metropolitan areas in Europe and North America is common knowledge. If a United Nations organization were responsible for ATC for 120 to 130 nations in the world, it is conceivable that as many as 84,000 commercial aircraft could require ATC in the twenty-first century. A rosette constellation of SBR satellites at an orbital altitude of 5600 nmi (10,371 km) in a 14/14/12 Walker orbit²³ inclined at 49.4° provides continuous worldwide visibility by at least two satellites simultaneously. (One satellite is deployed in each of 14 equally spaced orbit planes.) Each satellite provides radar coverage between grazing angles from 3 to 70°. The major subsystems in the satellite include (1) radar, (2) communications, (3) guidance and control, and (4) electrical power subsystems. Details of these subsystems are found in Ref. 12. The radar parameters are shown in Table 22.9. Each T/R module would have a peak power of 0.155 W and an average power of 15 mW and would weigh 5 g.

TABLE 22.9 Radar Parameters for Global Air Traffic Surveillance*

Antenna	
Type	Corporate-fed active phased array
Diameter	100 m
Frequency	2 GHz
Wavelength	0.15 m
Polarization	Circular
Number of elements	576,078
Number of modules	144,020
Element spacing	0.7244 wavelength
Beamwidth	1.83 mrad
Directive gain	66.42 dB
Maximum scan angle	22.4°
Receiver	
Type	Distributed solid-state monolithic T/R module
Bandwidth	500 kHz
System noise temperature	490 K
Compressed pulse width	2 μs
Transmitter	
Type	Distributed solid-state monolithic T/R module
Peak power	22.33 kW
Pulse width	2000 μs
Maximum duty	0.20
Frequency	2 GHz
Signal Processor	
Type	Digital
Input speed	50 million words per second

*From Ref. 12.

Military SBR Systems. Brookner and Mahoney¹¹ derived a satellite radar architecture for performing the basic surveillance missions for the fleet defense and air defense of the CONUS. The system was an L-band, corporate-fed phased array radar in orbit constellations of 3 to 12 satellites at altitudes from 600 to 2000 nmi. At the highest orbital altitude, a 10- by 30-m phased array that contained 15,000 radiating elements or modules was designed. The modules delivered an average power of 6 kW, and the radar required a prime power of 30 kW.

REFERENCES

1. Hughes Aircraft Company: "K_u-Band Integrated Radar and Communications Equipment for the Space Shuttle Orbiter Vehicle," preliminary design review, vol. 1, Mar. 14-24, 1978.
2. RCA Government and Commercial Systems, Aerospace Systems Division, Burlington, Mass.: "The Apollo LM Rendezvous Radar and Transponder," *Rept. LTM 3300-14D*, February 1971.
3. Quigley, W. W.: Gemini Rendezvous Radar, *Microwave J.*, pp. 39-45, June 1965.
4. Fenner, R. G., and R. F. Broderick: Spaceborne-Radar Applications, chap. 34 in Skolnik, M. I. (ed.): "Radar Handbook," McGraw-Hill Book Company, New York, 1970.
5. Elachi, C., et al.: Spaceborne Synthetic Aperture Imaging Radars: Applications, Techniques and Technology, *Proc. IEEE*, vol. 70, pp. 1174-1209, October 1982.
6. Elachi, C., and J. Granger: Spaceborne Imaging Radars Probe "in Depth," *IEEE Spectrum*, vol. 19, pp. 24-29, November 1982.
7. Williams, F. C., et al.: The Pioneer Venus Orbiter Radar, 1976 *WESCON Sess. 4*, Los Angeles, Sept. 14-17, 1976.
8. Hofmeister, E. L., et al.: GOES-C Radar Altimeter, vol. 1, "Data Users Handbook," General Electric Company, Utica, N.Y., May 1976.
9. Soviet Radar Records Venus Surface Imager, *Aviat. Week Space Technol.*, vol. 119, p. 18, Oct. 24, 1983.
10. Ulsamer, E.: In Focus—Approach Set on Space Radars, *Air Force Mag.*, vol. 67, pp. 17-18, February 1984.
11. Brookner, E., and T. F. Mahoney: Derivation of a Satellite Radar Architecture for Air Surveillance, *IEEE EASCON '83 Conf. Rec.*, Washington, Sept. 19-21, 1983.
12. Cantafio, L. J., and J. S. Avrin: Satellite-Borne Radar for Global Air Traffic Surveillance, *IEEE ELECTRO '82 Prof. Sess. Rec.*, Boston, May 25-27, 1982.
13. Cantafio, L. J.: Space Based Radar Concept for the Proposed United Nations International Satellite Monitoring Agency, *Mil. Microwaves Conf.*, London, Oct. 24-26, 1984.
14. "The Implication of Establishing an International Satellite Monitoring Agency," UN Publ. Sales No. E.83.IX.3.
15. Griffin, J. W., et al.: K_u-Band—The First Year of Operation, *IEEE Int. Radar Conf. Rec.*, pp. 330-339, Arlington, Va., May 6-9, 1985. (IEEE Cat. No. 85CH2076-8.)
16. Wolverton, R. W., et al.: "Flight Performance Handbook for Orbital Operations," John Wiley & Sons, New York, 1961.
17. Hord, R. A.: Relative Motion in the Terminal Phase of Interception of a Satellite or Ballistic Missile, *NACA TN 8399*, September 1958.
18. Functional Requirements for the Seasat-A Synthetic Aperture Radar System, *Jet Propulsion Lab., FR No. FM511774*, rev. dated Aug. 2, 1976, Pasadena, Calif.
19. "Geodynamics Experimental Ocean Satellite Project of the Earth and Ocean Physics

- Applications Program," NASA brochure, NASA Wallops Flight Center, Wallops Island, Va., 1975.
20. New Satellite to Measure Ocean Surface Topography and Sea State, *NASA News Release 75-88*, Washington, Mar. 31, 1975.
 21. GEOS-C Mission Plan, NASA TK-6340-001, rev. 3, NASA Wallops Flight Center, Wallops Island, Va., Dec. 18, 1974.
 22. Cantafio, L. J.: Satellite-Borne Radar, *Lecture IX, Adv. Radar Technol. Short Course*, scheduled by Technology Service Corporation, San Diego, Apr. 22, 1983.
 23. Walker, J. G.: Continuous Whole Earth Coverage by Circular Orbit Satellite Patterns, *R. Aircr. Estab. Tech. Rept. 77044*, Mar. 24, 1977.
 24. Luders, R. D., and L. J. Ginsberg: Continuous Zonal Coverage—A Generalized Analysis, *AIAA Pap. 74-842, AIAA Mech. Control of Flight Conf.*, Anaheim, Calif., Aug. 5-9, 1974.
 25. Ballard, A. H.: Rosette Constellation of Earth Satellites, *IEEE Trans.*, vol. AES-16, pp. 656-673, September 1980.
 26. Beste, D. C.: Design of Satellite Constellations for Optimal Continuous Coverage, *IEEE Trans.*, vol. AES-14, pp. 466-473, May 1978.
 27. Emara, E. T., and C. T. Leondes: Minimum Number of Satellites for Three-Dimensional Continuous Worldwide Coverage, *IEEE Trans.*, vol. AES-13, pp. 108-111, March 1977.
 28. Harney, E. D.: "Space Planners Guide," U.S. Air Force Systems Command, Publ. 0-774-405, 1965.
 29. Fager, J. A.: Application of Graphite Composites to Future Spacecraft Antennas, *AIAA Pap. 76-328, Sixth Commun. Satellite Syst. Conf.*, Apr. 6-8, 1976.
 30. Schultz, J. L., and P. Nosal: Space-Based Radar, *Horizons*, vol. 15, no. 1, p. 10, Grumman Aerospace Corporation, 1979.
 31. Fawcette, J.: Large Radar Satellite Proposed, *Microwave Syst. News*, vol. 8, pp. 17-20, September 1978.
 32. Mrstik, A. V., et al.: RF Systems in Space—Space-Based Radar Analysis, *General Research Corporation, RADC TR-83-91, Final Tech. Rept.*, vol. II, April 1983.
 33. Ludwig, A. C., et al.: RF Systems in Space—Space Antennas Frequency (SARF) Simulation, *General Research Corporation, RADC TR-38-91, Final Tech. Rept.*, vol. I, April 1983.
 34. Kendrick, J. B. (ed.): "TRW Space Data," 3d ed., 1967.
 35. Barton, D. K.: A Half Century of Radar, *IEEE Trans.*, vol. MTT-32, pp. 1161-1169, September 1984.
 36. Tu, K., et al.: Space Shuttle Communications and Tracking System, *Proc. IEEE.*, vol. 75, pp. 356-370, March 1987.
 37. Brejcha, A. G., L. H. Keeler, and G. G. Sanford: The Seasat-A Synthetic Aperture Radar Antenna, *Synth. Aperture Radar Technol. Conf.*, Las Cruces, N. Mex., Mar. 8-10, 1978.
 38. Kalmykov, A. I., et al.: Side-Looking Radar of Kosmos-1500 Satellite, *Issled. Zemli Kosmosa*, no. 3, May-June 1985.
 39. Soviets Plan to Launch New Spacecraft, *Aviat. Week Space Technol.*, vol. 127, p. 27, Oct. 19, 1987.
 40. Bearnse, S. V.: Knitted Antenna Solving Knotty Problems, *Microwaves*, p. 14, March 1974.
 41. Large Furlable Antenna Study, *Lockheed Missiles and Space Company, Rept. LMSC-D384797*, Jan. 20, 1975.
 42. Cummings, Freeman, and Benz: Deployable Parabolic Antenna, U.S. Patent 3,789,375, Dec. 18, 1973, assigned to Rockwell Inc.

43. Fager, J. A., and R. Garriott: Large Aperture Expandable Truss Microwave Antenna, *IEEE Trans.*, vol. AP-17, pp. 452-458, July 1969.
44. Das, A., and J. A. Delaney: Spacecraft Phased Array Configurations, *IEEE Trans.*, vol. AP-17, pp. 522-524, July 1969.
45. Final Report—Spaceborne Radar Study, *Grumman Aerospace Corporation, AFSC-ESD contract F19628-74-R-0140, Rept. 74-21AF-1*, June 28, 1974.
46. Hagler, T.: Building Large Structures in Space, *Astronaut. Aeronaut.*, vol. 14, pp. 56-61, May 1976.
47. Deployable Antenna Flight Experiment—Preliminary Definition Study, *Harris Corporation, Third Q. Rev.*, June 24, 1981.
48. Deployable Antenna Flight Experiment Definition Study: Mid-Term Review, *Grumman Aerospace Corporation, NAS-8-33932*, Mar. 20, 1981.
49. Bujakes, V. I., et al.: Infinitely Built-Up Radio Telescope, *Pap. IAF-77-67, IAF XXVIII Cong.*, Prague, Sept. 25-Oct. 1, 1977.
50. Ulsamer, E.: ATS-6, NASA's Huge Transmitter in the Sky, *Air Force Mag.*, vol. 57, August 1974.
51. Archer, J. S.: Advanced Sunflower Antenna Concept Development, *LSST First Ann. Tech. Rev.*, NASA LRC, Nov. 7-8, 1979.
52. Lockheed Tests Large Space Antenna, *Aviat. Week Space Technol.*, vol. 120, p. 70, Apr. 30, 1984.
53. Larson, T. R., A Microstrip Honeycomb Array for the Low Altitude Space Based Radar Mission, *Ball Aerospace Systems Division, Rept. F81-06*, August 1981.
54. Final Report—Spaceborne Radar Study, *Grumman Aerospace Corporation, Rept. 74-21-AF-1, prepared for ADSC-ESD (XRS) contract F19623-74-R-0140*, June 28, 1974.
55. Thimlar, M. E., et al.: Future Space-Based Computer Processors, *Aerosp. Am.*, vol. 22, pp. 78-82, March 1984.
56. Works, G. A.: Advanced Onboard Signal Processor, *IEEE EASCON '80 Rec.*, p. 233, 1980.
57. GaAs Solar Cells, *Hughes Aircraft Company, presented at Space Power Conf.*, Los Angeles, Jan. 13-14, 1981.
58. Emigh, C. R.: Reactor Technology, January-March 1980, *Los Alamos Scientific Laboratory, Prog. Rept. LA-8403-PR-UC-80*, June 1980.
59. Buden, D., et al.: Space Nuclear Reactor Power Plants, *LASL Informal Rept. LA-8223-MS-UC-33*, January 1980.
60. Buden, D., et al.: Selection of Power Plant Elements for Future Reactor Space Electric Power Systems, *LASL Rept. LA-7858*, September 1979.
61. Kelley, J. H.: Minutes of Space Nuclear Power Service Working Group Meeting, Sept. 24, 1982, issued Oct. 8, 1982.
62. Orbital Maneuvering Vehicle, *NASA George C. Marshall Space Flight Center, Request for Proposal 1-6-pp-01438*, November 1985.
63. Dietz, R. H.: Space Station Communications and Tracking Systems, *Proc. IEEE*, vol. 75, pp. 371-382, March 1987.
64. Carver, K. R., C. Elachi, and F. T. Ulaby: Microwave Remote Sensing from Space, *Proc. IEEE*, vol. 73, pp. 970-996, June 1985.
65. Bogomolov et al.: Venera 15 and 16 Synthesized Aperture Radar in Orbit around Venus, *Izv. Vyssh. Uchebn. Zaved., Radiofiz.*, vol. 28, pp. 259-274, March 1985.
66. NASA Announcement of Opportunity: The Earth Observing System (EOS), *A.O. No. OSSA-1-88*, Jan. 19, 1988.
67. Lorra/Tramar Design—Feasibility Study, *Malibu Res. and TRW*, MRA p. 214-3, May 11, 1988.